Ab initio study of the surface properties of austenitic stainless steel alloys

H. Pitkänen[a], M. Alatalo[a], A. Puisto[b], M. Ropo[c], K. Kokko[d,e], L. Vitos[f,g,h]

[a] *Department of Mathematics and Physics, Lappeenranta University of Technology, P.O.B 20, FIN-53851 Lappeenranta, Finland*
[b] *Aalto University, School of Science, Department of Applied Physics, P.O. Box 14100, FI-00076 AALTO, Finland*
[c] *Fritz-Haber-Institut, der Max-Planck-Gesellschaft, Faradayweg 4-6, D-14195 Berlin-Dahlem, Germany*
[d] *Department of Physics and Astronomy, University of Turku, FI-20014, Turku, Finland*
[e] *Turku University Centre for Materials and Surfaces (Matsurf)*
[f] *Applied Materials Physics, Department of Materials Science and Engineering, Royal Institute of Technology, SE-10044 Stockholm, Sweden*
[g] *Department of Physics and Astronomy, Division of Materials Theory, Uppsala University, Box 516, SE-751210 Uppsala, Sweden*
[h] *Research Institute for Solid State Physics and Optics, Wigner Research Centre for Physics, P.O. Box 49, H-1525 Budapest, Hungary*

Abstract

Using *ab initio* calculations we investigated the surface energies of paramagnetic $Fe_{1-c-n}Cr_cNi_n$ random alloys within the concentration range of $0.12 \leq c \leq 0.32$ and $0.04 \leq n \leq 0.32$. These alloys crystallize mainly in the face centred cubic (fcc) structure and constitute the main building blocks of austenitic stainless steels. It was shown that all alloys have the lowest surface energies along the most close packed crystal orientation, namely the fcc (111) surfaces. The amount of Ni seems to have little effect on the surface energy, while almost all composition-driven change may be attributed to the changes in the Cr content. Within the studied compositional range, the change of the surface energy with the composition is of the order of 10%. Some phenomena found for surface energy can be related to the magnetic structure of surfaces. Using the total energy as a function of the concentration, the effective chemical potentials in bulk and at the surface can be determined, and from them, the surface segregation energies.

Keywords:

Stainless steel, Surface energy, First-principles calculation, FeCrNi, Austenitic, Alloy surface

1. Introduction

Stainless steels are the most widely used maintenance free and safe engineering materials. They have superior strength, stiffness, toughness and corrosion resistance in relation to their cost compared to other materials. Surface energy is one of the defining qualities of Fe alloys, because it determines many important phenomena, such as crystal growth, adhesion between metallic surfaces, growth of thin layers [1], and mechanical strength. Surface energies of solids can not be directly measured; instead, the available "experimental" surface energies have been derived from liquid tension measurements. Therefore theoretical studies on the subject are of vital importance to the development of this field.

In this work, the surface energies of austenitic FeCrNi alloys (with varying Cr and Ni concentrations) were calculated. The crystal structure of these alloys was the face centered cubic (fcc) lattice. The two low index surfaces, fcc(100) and fcc(111) were studied, because they are the most closely packed ones, and thus the most likely candidates to have the lowest surface energy.

The minimum Cr amount in our study was chosen to be 12% (atomic % is used throughout the report), given by the stainless requirement [2], and the maximum 32%. Since almost all stainless steels contain at least some Ni, we chose the lower limit of Ni to be 4% corresponding to some metastable grades present e.g. in duplex steels. Since Ni also has a stabilizing effect on the austenitic phase, we mimic the effect of all austenite stabilizers by Ni. Therefore, we chose the upper limit for Ni to be as high as 32%, even though such an amount of Ni is not commonly used in any commercial steel grades.

The paper is organized as follows: In section 2 the computational methods of calculating the surface energies are introduced and discussed. In section 3 we display the results, and finally, in chapter 4, the conclusions are presented.

2. Methods

2.1. Surface energy

Cutting a solid body into two disrupts its bonds, and therefore consumes energy. This additional energy fed into the system when the bonds are cut is called the surface energy, and it is expressed as energy per surface area. To acquire the surface energy via simulations, we considered two systems per each composition (varying c and n in $Fe_{1-c-n}Cr_cNi_n$), namely a slab system and a bulk system. The slab system consisted of eight atomic layers, separated by a vacuum of 4 atomic layers thickness. Both the width of the slab and the width of the vacuum layer were chosen to be adequate for the material to attain bulk-like behavior in the middle of the slab, and for the surfaces to not be interfered by the repeated images (that is, they react as if exposed to infinite void, not to a small crack). The exact coordinates used for both the fcc(111) and fcc(100) case can be found as supplementary material (online publication). The amount of "surplus energy" (surface energy) in the system is the total energy of the slab system minus the energy of the bulk system having the same amount of atoms as the slab system has. Mathematically, the surface energy is expressed as

$$\gamma = \frac{E_{\text{slab}} - n \cdot E_{\text{bulk}}}{2A}, \tag{1}$$

where E_{slab} is the total energy of the slab system, n is the number of atoms in the slab system, E_{bulk} is the energy per atom of the bulk system, and A is the area of an interface in the slab supercell. The "2" in the denominator stands for the two surfaces of the slab. It is worth mentioning here, that the surface of any alloy consisting of two or more different chemical elements assumes a certain surface chemical concentration profile which depends on the elements of the alloy and the surface considered. They might form a dilute alloy, or one of the elements might segregate to the surface, and the elements on the surface can form islands of varying shapes and sizes. Such phenomena are not considered here. Therefore, in the present study, the surfaces are in their bulk concentrations. We determined the equilibrium lattice parameter for each composition (that is, for each c and n in $Fe_{1-c-n}Cr_cNi_n$) by performing a series of total energy calculations with a varying lattice parameter value, and then fitting a Morse equation of state to the *ab initio* total energies. The obtained theoretical volume (lattice parameter) was then adopted in

the slab calculations. The variation in the lattice parameter was very small in the studied compositional range: the difference between smallest (3.6032 Å) and largest (3.6111 Å) value was 0.22%.

There are various ways one can use to define the bulk total energy, which is then used as a reference energy when calculating the surface energies (defined in Eq. 1). One possibility is to use as the bulk reference energy the total energy difference between two slabs consisting of N+1 and N atomic layers. Another solution is to use the same supercell (without vacuum layers) to compute the bulk energy as the one used for the slab calculation. Finally, one could limit the size of the slab to the minimum thickness and use the separate bulk total energy in the calculation. In this case the error due to the different sampling of the bulk and slab Brillouin zones can also be kept at minimum. We adopted the third approach for our simulations. Moreover, Florentini *et al.* [4]) showed that the difference in obtained surface energy between the described methods is in the range of 1-2%. That accuracy is enough for our purposes.

The convergence of the surface energies as a function of slab thickness was not tested as a part of this work, but previous surface energy studies [3] demonstrated that for the present close-packed surfaces 8 atomic layers give converged results. Also, Florentini *et al.* [4]) showed that the obtained surface energy value between the various methods discussed in the last paragraph diverges with slab thickness, the methods being most consistent with each other when slab thickness is between 6-8 layers.

2.2. Computational details

For an adequate simulation of paramagnetic alloy steels both the chemical and magnetic disorder should be treated simultaneously [5]. In the present application, we modeled the bulk $Fe_{1-c-n}Cr_cNi_n$ system by an alloy with randomly distributed chemical species and local magnetic moments, *i.e.* by a four component random $Fe^{\uparrow}_{(1-c-n)/2}Fe^{\downarrow}_{(1-c-n)/2}$ Cr_cNi_n alloy. Here the arrows represent the two magnetic moments oriented up (↑) and down (↓). This disordered local moment (DLM) approach accurately describes the effect of loss of the net magnetic moment above the transition temperature [6]. Unlike in the bulk, the magnetic moments of Cr tend to split near the surface. Thus, for the slab system, instead of the four component alloy $Fe^{\uparrow}_{(1-c-n)/2}Fe^{\downarrow}_{(1-c-n)/2}$ Cr_cNi_n we have to use a six component alloy

$Fe^{\uparrow}_{(1-c-n)/2}Fe^{\downarrow}_{(1-c-n)/2}Cr^{\uparrow}_{c/2}Cr^{\downarrow}_{c/2}Ni^{\uparrow}_{n/2}Ni^{\downarrow}_{n/2}$. We should mention that in the paramagnetic state, the bulk and surface Ni atoms become polarized only if one takes into account the thermal (longitudinal) spin fluctuations. This is beyond the scope of the present work. On the other hand, Cr atoms show a much stronger surface moment enhancement (already in elementary Cr; [23]), which might explain why Cr has non-vanishing local magnetic moment at the surface.

Here we exclusively considered homogeneous substitutionally disordered FeCrNi alloys, without interstitials and precipitates. Also the effects of short range order and relaxation effects were omitted. It is well known that interstitial C and N have a strong effect on stabilizing the austenitic phase. However, modeling the effect of interstitials from the first principles theory is very cumbersome especially in the chemically and magnetically disordered matrix. For this reason, we mimic the effect of all austenite stabilizers with Ni, as mentioned earlier.

The most straightforward way to compute the total energy of a disordered alloy system would be to construct a large supercell with randomly distributed solute atoms. However, in the case of an alloy with four or even six components, the supercell would have to be huge, and thus calculations based on that would cause noticeable computational cost. It is worth pointing out that one would have to perform several such calculations for each composition in order to average over different configurations. There is, however, a more novel way to calculate the total energies of random substitutional alloys, with far smaller computational cost. In this study, we employed the Coherent Potential Approximation (CPA) [7], in which the alloy components are embedded in an effective medium, which is constructed in such a way that it represents, on the average, the scattering properties of the alloy. In the present application, we adopted the CPA implemented within the framework of the Exact Muffin-Tin Orbitals (EMTO) method [8, 5].

The EMTO method is an improved screened Korringa-Kohn-Rostoker method [9], where the one-electron potential is represented by large overlapping muffin-tin potential spheres. By using overlapping spheres, the crystal potential can be described more accurately, when compared with the conventional non overlapping muffin-tin approach [10, 11, 12].

The FeCrNi alloys form the basis of the austenitic stainless steels. These alloys are paramagnetic at room temperature having sizable (disordered) local magnetic moments. However, these theoretical local moments depend sensitively on the volume. Soft-core calculations yield equilibrium volumes which are substantially smaller than those observed in experiment. The obvious reason for this discrepancy is the thermal expansion, which has been neglected in the present theoretical study. The unusually large thermal expansion originates from the fact that the paramagnetic fcc Fe (and also the present alloys) shows a magnetic transition near the equilibrium volume [13]. As a consequence, a straightforward soft-core calculation cannot capture the proper magnetic state of the present alloys. (We should also mention that both the local- and the gradient-level density functional approximations underestimate the equilibrium volume of magnetic 3d metals and thus further increase the above error.) One possibility to overcome this difficulty is to perform frozen-core calculations, which yield larger equilibrium volumes and thus better account for the paramagnetic state. This is why all our calculations have been performed within the frozen-core scheme.

All calculations in the present work were carried out using the generalized-gradient approximation [14] for the exchange-correlation density functional. The EMTO basis set included s, p, d, and f orbitals. The one-electron equations were solved within the scalar-relativistic approximation. For each composition and crystal lattice, the EMTO Green's function was calculated self-consistently for 16 complex energy points distributed exponentially on a semi-circular contour, which included states within 1 Ry below the Fermi level. In the one-center expansion of the full charge density, we adopted an l-cutoff of 10 and the total energy was calculated using the Full Charge Density technique [11, 5, 16]. The **k**-points were distributed uniformly, using a $13 \times 13 \times 1$ mesh in slab and a $17 \times 17 \times 17$ mesh in bulk calculations [15].

3. Results and Discussion

3.1. Surface energies

Figure 1 shows the surface energy of the fcc(111) surface. As can be noted, the amount of Ni has little effect on the surface energy, whereas increasing the amount of chromium from 12% to 32% raises the surface energy from around 2.7 J/m^2 to 3.0 J/m^2. Figure 2 shows the surface energy of the fcc(100) surface. Compared to the case of the fcc(111) surface, the energy is

somewhat higher in the whole composition range. As in the case of fcc(111), the amount of Ni has far less effect on the surface energy than Cr.

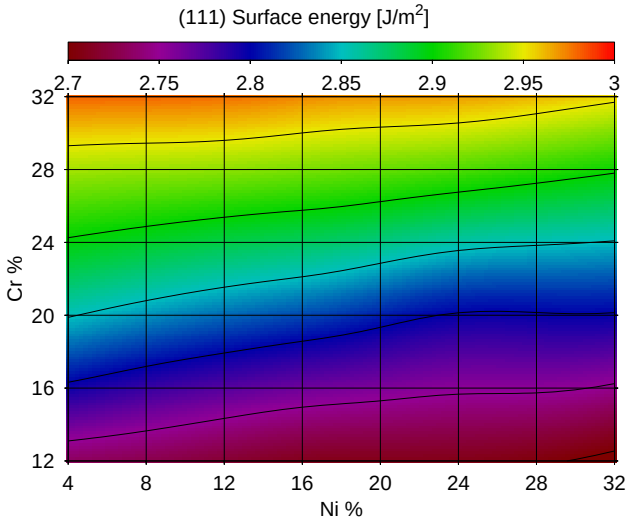

Figure 1: Surface energy of FeCrNi(111). Spacing between contours is .05 J/m^2.

Jun Yu *et al.* [1] simulated the surface energy of $Fe_{23}Cr_6Ni_3$ using the supercell approach, and obtained 2.08 J/m^2 for the fcc(111) surface and 2.06 J/m^2 for the fcc(100) surface. Our values for that composition are 2.8 J/m^2 for fcc(111) and 3.1 J/m^2 for fcc(100). The differences between our results and those of Jun Yu *et al.* are explained by the fact that we use different methods. Their approach utilizes the supercell method (this affects chemical disorder), and also, their approach excludes any magnetic effects. We could make a comparison to the estimated surface energy of pure Fe, obtained from liquid surface tension measurements (around 2.4 J/m^2 [17]), but since clean Fe is bcc and ferromagnetic, whereas our case is an fcc paramagnetic system and Jun Yu *et al.* worked with a non-magnetic fcc system, the comparison is of little use. Punkkinen *et al.* [18, 19] simulated the surface energy of ferromagnetic bcc Fe using the supercell method, and obtained a value of 2.45 J/m^2 for bcc(110). Jun Yu *et al.* got, employing the GGA-PBE approximation, 2.435 J/m^2 for the relaxed bcc(100) surface, 2.370 for J/m^2 the relaxed bcc(110) surface, 3.239 J/m^2 for the unrelaxed bcc(100) surface and 3.012 J/m^2 for the unrelaxed bcc(110) surface. However, Punkkinen *et al.* did not find any significant relaxation for bcc ferromagnetic Fe, in contrast to the huge relaxations reported by Jun Yu *et al.*

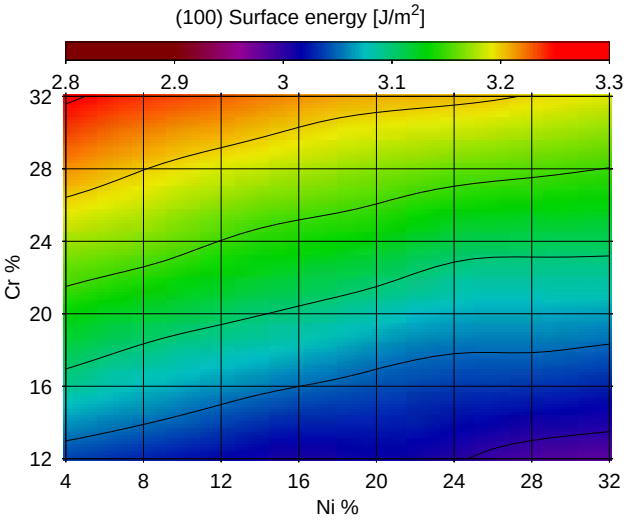

Figure 2: Surface energy of FeCrNi(100). Spacing between contours is .05 J/m^2.

Clean Cr is paramagnetic, so it has nonzero magnetic moments both in the bulk and in the surface. Aldén *et al.* [20, 21] have found, in their investigations on the surface energies of 3d transition metals in magnetic and nonmagnetic state, that the surface energy of nonmagnetic fcc(111) Cr is 7% (15%) higher than the surface energy of magnetic fcc(111) Fe (magnetic fcc(111) Ni). Their studies [21], as well as those of Punkkinen *et al.* [18], also show that the spin polarization of Cr decreases the surface energy of bcc(100) Cr by 20-30%.

We found (Table 1) that the magnetic moments of Cr are smaller in a FeCrNi surface, than they are in a FeCr surface [22] or a clean Cr surface [21] (this is true for both (111) and (100) surface orientations). This suggests that the increasing of the surface energy of FeCrNi alloys with increasing Cr content is related to the reduced magnetic moment of Cr at FeCrNi surfaces compared to those of FeCr or clean Cr. This argument is supported further by noting that the magnetic moments of Cr are smaller in the fcc(111) surface compared to those in the fcc(100) surface, and correspondingly, the obtained Cr enhancement of the surface energy is stronger for the fcc(111) surface than for the fcc(100) surface (this is easily observed when looking at the surface energy parametrization equations shown in subsection 3.4). The effect of Cr

to increase the surface energy seems to be a rather robust effect in Fe-alloys since adding Cr to ferritic FeCr alloys similarly increases the surface energy of the (100) surface [22].

3.2. Surface magnetism

Magnetic moments of Fe and Cr versus layer depth are listed in table 1. Magnetic moments of Ni are omitted from the table, as they are all zero. The magnetic moments of Fe increase from their bulk values of around 1.6 μ_B to 2.5 μ_B for the (100) surface and to 2.2 μ_B for the (111) surface. These findings are in line with those of Ohnishi *et al.* [24]. A peculiarity one notices about the magnetic moments of Fe in this table is the fact that the 4th layer values (the 4th layer represents bulk in this calculation, as 8 layers was thought to be enough for convergence) are not the same for (100) and (111). If 8 layers were enough for the magnetic behavior to converge to bulk values in both cases, the values would be the same. This is also in line with the findings of Ohnishi *et al.* [24]; they used a slab 7 atomic layers thick, and noticed Friedel-type oscillations in the magnetic polarization throughout the entire slab. The fact that our method does not allow atoms to move from their theoretical lattice positions might also provide an explanation to this: since any driving forces can not move the atoms, magnetic frustrations might be formed. The 4th layer value for the (100) slab is very close to the one acquired via a bulk calculation with this method, 1.65 μ_B. In the (111) case, the magnetic moment deviates 6.7% from its bulk value.

As mentioned earlier, the magnetic moments of Cr were assumed not to split in the central layers, and split only in the surface layer, and possibly in the 2nd. This turned out to be the case. Kiejna *et al.* [25], as well as Ropo *et al.* [22] arrived to a similar conclusion in their study of bcc FeCr alloys. Kiejna *et al.* also studied how the magnetic moment of Cr changed depending on the surface geometry, and arrived to the conclusion that when Cr atoms have the largest number of bonds missing (because they reside at the surface), magnetic moment is the largest, as seen also in our study (Table 1).

3.3. Surface energy anisotropy

Figure 3 shows the surface energy of the (100) surface divided by that of the (111). The higher the value, the more likely the material is to break

		(100)	(111)
Surf	Fe	2.54	2.16
	Cr	2.32	1.04
2nd	Fe	1.76	1.57
	Cr	0	0
3rd	Fe	1.66	1.54
	Cr	0	0
4th	Fe	1.67	1.54
	Cr	0	0

Table 1: Magnetic polarization of Cr and Fe as a function of the distance from surface. The numbers are reported in Bohr magnetons. Magnetic polarization changed very little (almost not at all) in the entire concentration range studied. The reported values are at composition: 16% Cr, 16 % Ni, rest Fe. Corresponding magnetic moment (using this same method) for bulk is 1.65 μ_B.

along the alignment with lower surface energy. A value of 1 would mean that both are equally likely. As we can see, the anisotropy does not change much with concentration. Chromium has almost no effect on it at all, and with Ni the change is only in the order of 1%. In a simple bond cutting model, the surface energies for the three low-index fcc surfaces are roughly proportional to the number of removed nearest neighbor atoms per surface area when the surface is created. The anisotropy ratio given by the bond cutting model is 1.15, which is fairly close to our reported values.

Jun Yu *et al.* [1] acquired for $Fe_{23}Cr_6Ni_3$ alloy, using the supercell approach, a surface energy anisotropy dissimilar to ours. Our results indicate that the fcc(111) surface is lower in energy in the entire concentration range studied; however, their result was the opposite. The explanation for this discrepancy might lie in the following factors: first of all, the surface chemical composition Jun Yu *et al.* use is not the same for fcc(100) and fcc(111). Second, their analysis excludes the effect of magnetism, which is reflected on the rather imprecise values they got for equilibrium volume and bulk modulus. In our case, the chemical compositions were exactly the same, and magnetic effects were included (within the DLM scheme).

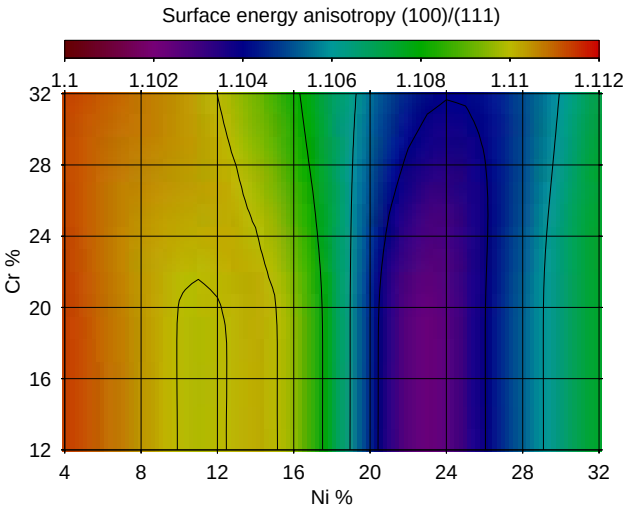

Figure 3: Surface energy anisotropy: $\gamma(100)$ / $\gamma(111)$. Line separation is 0.002.

3.4. Parametrization of surface energy

By fitting a simple planar function of the form $f(c, n) = ac+bn+d$, where n and c are the amounts of Ni and Cr in the alloy, respectively (in atomic fractions), to the sets of points we used to plot Figs. 1-2, we can estimate how the surface energy behaves as a function of c and n. The estimate functions are as follows:

$$\begin{aligned} \gamma(111) = &\quad 1.279 \cdot c \quad -0.143 \cdot n + 2.588 \quad [\mathrm{J/m^2}] \\ \gamma(100) = &\quad 1.042 \cdot c \quad -0.228 \cdot n + 2.926 \quad [\mathrm{J/m^2}], \end{aligned}$$

where the variables are within the limits ($0.12 \leq c \leq 0.32$, $0.04 \leq n \leq 0.32$).

As we can see when comparing Figs 1 and 2, the amount of Ni has more effect on the surface energy in the case of (100) surface as compared to the (111) surface. That can also be clearly seen in the estimate functions when comparing the coefficients of n in both cases. Also, the surface energy was a bit higher in the whole composition range for the (100) surface, which can again be seen when looking at the constant terms of the functions. The fact that the amount of Cr affects the surface energy more than the amount of Ni is obvious, looking at the coefficients of c and n.

3.5. Surface segregation tendencies of alloy component

To support our study of surface energies we estimated the difference between the Cr and Ni chemical potentials (effective chemical potential) in the bulk and in the (111) surface for a homogeneous FeCrNi alloy containing 20% Cr and 16% Ni. The effective chemical potential for each component is defined by

$$\Delta\mu_{\text{eff}}^{X=Cr,Ni} = \frac{\delta E}{\delta c_X} \ , \tag{2}$$

where $\Delta\mu_{\text{eff}}^{X}$, E and c_X are effective chemical potential, energy per atom and the concentration of component X, respectively. That is, the effective chemical potential is the partial derivative of the free energy with respect to the concentration. In our simulations, when the amount of Cr was changed, the amount of Ni was held fixed, and vice versa.

The estimated effective chemical potentials are as follows. For Ni they are $\Delta\mu_{\text{eff,bulk}}^{\text{Ni}}$ = -35.283 Ry in the bulk, and $\Delta\mu_{\text{eff,surf}}^{\text{Ni}}$ = -35.303 Ry in the surface. For Cr they are $\Delta\mu_{\text{eff,bulk}}^{\text{Cr}}$ = 23.199 Ry in the bulk and $\Delta\mu_{\text{eff,surf}}^{\text{Cr}}$ = 23.221 Ry in the surface.

As surface segregation energies can be obtained by taking differences in effective chemical potential between bulk and surface, we see that Ni has a tendency to segregate towards the surface ($\Delta\mu_{\text{eff,surf}}^{Ni} - \Delta\mu_{\text{eff,bulk}}^{Ni}$ = -20mRy), whereas for Cr it seems to be energetically more favourable to segregate towards the bulk ($\Delta\mu_{\text{eff,surf}}^{Cr} - \Delta\mu_{\text{eff,bulk}}^{Cr}$ = 22mRy). This is in agreement with the trends we can see in Figs 1 and 2: with increasing Cr content the surface energy increases, and with increasing Ni content the surface energy decreases.

As it is Cr that makes stainless steels stainless by forming a protective layer to its surface, it might seem counterintuitive at first to realize that Cr tends to segregate towards the bulk, and Ni to the surface. However, there is no discrepancy here. Jussila *et al.* [26] studied the surface of FeCrNi by measurements, and found that when annealed, Ni is enriched at the surface (in accordance with our results) and due to higher affinity to oxygen it is Cr oxide that is found at the surface, when the surface is brought to contact with an oxygen containing atmosphere. Later also Fe oxide is found (due to higher mobility of Fe ions).

4. Conclusions

Our main result is the *ab initio* database of the surface energy versus composition. Increasing the Cr content by one atomic percent while keeping Ni content fixed increases the surface energy with approximately 11 mJ/m^2. On the other hand, increasing Ni content by one atomic per cent (Cr content fixed) decreases the surface energy with approximately 2 mJ/m^2. The enhancement of surface energy with increasing Cr content is shown to have, at least to a certain degree, a magnetic origin.

The order of surface energy versus surface orientation is such, that the more closely packed the surface is, the smaller is the surface energy (our ongoing study shows that the same trend continues to the (110) surface). This is a normal surface anisotropy, which is characteristic to most of the late transition metals. However, the fact that a single crystal alloy has as the most stable surface the (111) facet, may not have any substantial implications to the real alloys. In normal conditions, steels are never seen as a single crystal, rather, they have a macro structure consisting of grains of varying sizes, each with a different crystal alignment. If we imagine a real life situation of a steel breaking, different grains will break along different crystal alignment planes, and thus the most realistic candidate for the energy it takes to cleave a steel bulk in a real situation is acquired by averaging several single grain surface energies.

5. Acknowledgements

We wish to gratefully acknowledge the Academy of Finland (Research Grant #115362), and the LUT Foundation. CSC, The Finnish IT center for Science, is acknowledged for their computational resources. L.V. acknowledges support from the Swedish Research Council, the Swedish Steel Producers Association, the European Research Council and the Hungarian Scientific Research Fund (research project OTKA 84078).

[1] Yun Ju, Xin Lin, Jungie Wang, Jing Chen, and Weidong Huang, Appl. Surf. Sci. 255 (2009) 9032-9039.

[2] G. Wrangler, An introduction to Corrosion and Protection of Metals, Chapman and Hall, London (1985).

[3] L. Vitos, A.V. Ruban, H.L. Skriver, J. Kollár, Surf. Sci. 411 (1998) 186.

[4] V. Fiorentini, M. Methfessel, Extracting convergent surface energies from slab calculations, J. Phys. Condens. Matter 8 (1996) 6525.

[5] L. Vitos, in Computational Quantum Mechanics for Materials Engineers: The EMTO Method and Applications, Engineering Materials and Processes Series (Springer-Verlag, London, 2007).

[6] J. Staunton, B. L. Györffy, A. J. Pindor, G. M. Stocks, H. Winter, J. Magn. Magn. Mater. 45 (1984) 15; B. L. Györffy, A. J. Pindor, J. Staunton, G. M. Stocks, H. Winter, J. Phys. F: Met. Phys. 15 (1985) 1337.

[7] P. Soven, Phys. Rev. 156 (1967) 809-813; B. L. Györffy, Phys. Rev. B 5 (1972) 2382-2384.

[8] L. Vitos, I.A. Abrikosov, and B. Johansson, Phys. Rev. Lett. 87 (2001) 156401.

[9] O.K. Andersen, O. Jepsen, and G. Krier, in Lectures on Methods of Electronic Structure Calculations, ed. V. Kumar, O. K. Andersen, and A. Mookerjee, World Scientific Publishing Co., Singapore (1994) p. 63.

[10] O.K. Andersen, C. Arcangeli, R.W. Tank, T. Saha-Dasgupta, G. Krier, O. Jepsen, and I. Dasgupta, in Mat. Res. Soc. Symp. Proc. 491 (1998) p. 3.

[11] L. Vitos, Phys. Rev. B 64 (2001) 014107.

[12] L. Vitos, H. L. Skriver, B. Johansson, and J. Kollár, Comp. Mat. Sci. 18 (2000) 24.

[13] H. Zhang, B. Johansson, L. Vitos: Density Functional Study of Paramagnetic Iron, Phys. Rev. B. 84, 140411(R) (2011).

[14] J. P. Perdew, K. Burke, and M. Ernzerhof, Phys. Rev. Lett. 77 (1996) 3865.

[15] H. J. Monkhorst and J. D. Pack, Phys. Rev. B 13 (1976) 5188.

[16] J. Kollar, L. Vitos, H.L. Skriver, in: H. Dreyssé (Ed.), Electronic Structure and Physical Properties of Solids: The Uses of the LMTO Method, Lecture Notes in Physics, Springer-Verlag, Berlin (2000) pp. 85-113

[17] W. R. Tyson and W. A. Miller, Surf. Sci., 62 (1977) 267-276.

[18] M. P. J. Punkkinen, S. K. Kwon, J. Kollár, B. Johansson and L. Vitos, Phys. Rev. Lett. 106 (2011) 057202.

[19] M. P. J. Punkkinen, Q. Hu, S. K. Kwon, B. Johansson, J. Kollar, and L. Vitos, Phil. Mag. 91 (2011) 3627.

[20] M. Aldén, H. L. Skriver, S. Mirbt, B. Johansson, Phys. Rev. Lett. 69 (1992) 2296.

[21] M. Aldén, H. L. Skriver, S. Mirbt, B. Johansson, Surf. Sci. 315 (1994) 157.

[22] M. Ropo, K. Kokko, E. Airiskallio, M. P. J. Punkkinen, S. Hogmark, J. Kollár, B. Johansson and L. Vitos, J. Phys.: Condens. Matter. 23 (2011) 265004.

[23] M. Aldén, S. Mirbt, H. L. Skriver, N. M. Rosengaard, B. Johansson, Phys. Rev. B 46 (1992) 63036312.

[24] S. Ohnishi, A. J. Freeman, and M. Weinert, Phys. Rev. B 28 (1983) 12.

[25] A. Kiejna and E. Wachowicz, Phys. Rev. B 78 (2008) 113403.

[26] P. Jussila, K. Lahtonen, M. Lampimäki, M. Hirsimäki and M. Valden, Surf. Interface Anal. 40 (2008) 1149-1156.